Published online August 1, 2007

Vadose Zone Journal ORIGINAL RESEARCH

Geoelectric Studies of Seasonal Wetting and Drying of a Texas Vertisol

Sikiru A. Amidu* and John A. Dunbar

Vertisols are complex soils with high clay content (>30%), high shrink–swell potential, and microrelief features known as *gilgai*. We applied field and laboratory electrical-resistivity measurements to characterize seasonal wetting and drying of a Texas Vertisol, and to quantify the effects of gilgai and cracks on seasonal hydrodynamics of the soil. Thirty-two multielectrode resistivity-profiling lines were collected along the same profile from 1 May 2005 to 22 Apr. 2006, using combined dipole–dipole and Schlumberger electrode configurations. The profiles were 17.5 m long and intersected two sets of microlows and microhighs of the gilgai. The resistivity data were inverted using the RES2DINV program and the inverted data were corrected for temperature. We measured variations of resistivity with soil moisture in the laboratory and the results were used to calibrate the field data. To evaluate the resistivity results, in situ measurements of soil moisture were made using auger sampling. During the wetting cycle, three distinct soil moisture regimes were recognized in the upper 1.4 m of the Vertisol: an upper zone (0–0.5-m depth), which is the most dynamic with regard to wetting and drying; a middle zone (0.5–1.1 m), which is relatively saturated and less dynamic; and a lower zone (below 1.1 m), which is relatively less saturated compared with the middle layer. The saturation of the middle layer appears to be enhanced by preferential flow through cracks. Also, the microrelief topography exercises a control on spatiotemporal variations in soil moisture in that the microhighs dry faster than the microlows.

Accurate knowledge of seasonal wetting and drying of expansive clay soils such as Vertisols is important in understanding the mechanisms of shrinking and swelling and choosing the best agricultural and management practices for long-term sustainability of the soils. Vertisols cover about 308 million ha globally and 12 million ha in 25 states of the USA (Coulombe et al., 1996). In Texas, they cover about 6.5 million ha (Coulombe et al., 1996). Vertisols are characterized by high clay content (>30%) and a high shrink–swell potential. Their shrink–swell characteristics give rise to microtopographic expression of subsurface soil dynamics known as *gilgai* and deep cracks that may extend >1 m. Gilgai consists of a series of microhighs that are the higher parts of the microrelief, depressions or microlows that are the lower parts of the microrelief, and shelves that are planar or subplanar areas intermediate in elevation between the two other elements (Coulombe et al., 1996). Although these features form naturally in Vertisols over decades (Mermut et al., 1996), the exact mechanism by which they form is not well understood (Gustavson, 1975; Wilding and Tessier, 1988). Once developed, individual microhigh and microlow features may be >4 m wide and the elevation difference between adjacent peaks and troughs may be >0.3 m. It is known empirically that gilgai strongly influences the spatial pattern of water infiltration and soil moisture in Vertisols. For example, differences in plant growth in some cereal crops have been correlated to different gilgai elements (Wilding et al., 1991).

Soil moisture regimes in Vertisols are also influenced by deep cracks in the soils. In the U.S. Soil Taxonomy, the criteria used to divide Vertisols according to udic and udic–ustic soil moisture regimes are the duration and pattern of soil cracking (Dudal and Eswaran, 1988). The descriptions of cracking patterns as contained in these criteria are subjective, however, and the extent to which they reflect the climatic conditions under which Vertisols occur and which land management and utilization decisions are made is not clear (Dudal and Eswaran, 1988). Among identified acute areas of needed Vertisol research are verification of cracking patterns and cracking depths as a function of seasonal soil moisture between microhigh and microlow gilgai elements (Wilding et al., 1991; Newman, 1986).

Many recent studies of Vertisols have been performed in an attempt to understand soil moisture dynamics in these soils (e.g., Favre et al., 1997; Lin et al., 1997, 1998). There is no general agreement among the researchers, however, on concepts such as seasonal water fluxes, seasonal cracking patterns and their duration, and closure of cracks in response to soil wetting. For example, Favre et al. (1997) observed that on some cracked plots

Dep. of Geology, Baylor Univ., One Bear Place #97354, Waco, TX 76798-7354. Received 11 Jan. 2007. *Corresponding author (Sikiru_Amidu@baylor.edu).

Vadose Zone J. 6:511–523
doi:10.2136/vzj2007.0005

in a Vertisol of Senegal, surface irrigation and simulated rainfall resulted in crack closure within 4.5 h. They concluded that for the Vertisol studied, bypass flow through cracks would have little impact on the seasonal field water balance. Lin et al. (1997) performed infiltration studies on some soil samples from Vertisols in Texas. Their results suggested that low-tension (preferential) flow through macropores is an important process in the soils. Favre et al. (1997) also showed that crack closures start from the soil surface and progress downward; this contradicts the widely held view that closure of cracks starts from the bottom and progresses to the soil surface (e.g., Bouma and Loveday, 1988).

In general, characterizing soil moisture in Vertisols is an unfinished challenge (Wilding and Puentes, 1988). Precise characterization of soil moisture in Vertisols requires noninvasive two-dimensional (and three-dimensional) high-resolution and in situ monitoring of seasonal wetting and drying of the soils. Conventional methods of soil moisture measurements provide information of soil properties at a point and are destructive, making it difficult to carry out repeated measurements at the same locations. Geophysical methods offer a potential alternative that gives good spatial coverage but lower resolution. Ground penetrating radar is not applicable in this case, however, because high conductivity of clay soils limits signal penetration (Davis and Annan, 1989).

Electrical resistivity techniques are noninvasive and empirical relationships exist between resistivity and soil moisture for clay soils (Bussian, 1983; Frohlich and Parke, 1989). The techniques have been used in identifying subsurface structures (Griffith and Barker, 1993) and in mapping soil structure horizonation (Tabbagh et al., 2000) and soil pollution (Halvorson and Rhoades, 1976; Amidu and Olayinka, 2006). Michot et al. (2003) used the method in precision agriculture for monitoring water uptake by plants, whereas Besson et al. (2004) used the method to investigate the effects of tillage on soil properties. Recently, Samouëlian et al. (2003) discussed the potential for use of the method for characterizing cracks in soils. Also, because of the sensitivity of electrical resistivity to soil moisture, Hagrey and Michaelsen (1999), Zhou et al. (2001), and Garambois et al. (2002), among others, have characterized soil hydrology using these techniques.

In this study, we applied field and laboratory electrical resistivity measurements to characterize the seasonal wetting and drying of a Texas Vertisol and to quantify the effects of gilgai and cracks on soil moisture variations in the soil. We carried out laboratory measurements on soil samples and used the results to calibrate data from field two-dimensional resistivity surveying during wetting and drying cycles in the Vertisol. We evaluated the results of resistivity measurements by comparing with the results of soil moisture measurements by auger sampling. Finally, we related our results to in situ wetting and drying properties of the Texas Vertisol.

Materials and Methods

Site Description

The field site for this study is located at the USDA Grassland Soil and Water Research Station, near Riesel, TX (Fig. 1). The area is underlain by marls and chalks belonging to the Taylor Group of the Gulfian series of the Cretaceous system (Soil Conservation Service, 1942). These chalks and marls weather easily to develop soils that strongly reflect the character of the geologic material from which they are formed. The field site is on Houston Black soil within the research station (Fig. 1). In this area, Houston Black soils are classified as fine, montmorillonitic, thermic Udic–Ustic Haplusterts (Natural Resources Conservation Service, 2001; Soil Survey Staff, 1999). These soils exhibit strong shrink–swell potential, and microrelief gilgai features are well developed. Typical elevation difference between peaks and troughs of adjacent microlows and microhighs ranges from 10 to 30 cm, with horizontal spacing of 2 to 5 m. The landscape is characterized by gently rolling slopes ranging from 1 to 3% and soil thickness ranging from 1 to 3 m (Allen et al., 2005). The annual average precipitation is 787. 4 mm and the temperature ranges from a mean minimum of 2.2°C in January to a mean maximum of 36.1°C in July.

Theoretical Concepts

Soil is a three-phase system consisting of grain matrix, air, and water. With regard to electrical current conduction, soil water is the most important (Saarenketo, 1998). The commonly used relationship between resistivity and soil moisture is expressed as (Archie, 1942)

$$\rho_a = a\Phi^{-m}S^{-n}\rho_w \qquad [1]$$

where a, m, and n are petrophysical constants that are characteristic of the porous medium, ρ_a is the resistivity of the porous medium, ρ_w is the pore-water resistivity, Φ is the porosity, and S is saturation, which is the ratio of the water content and porosity.

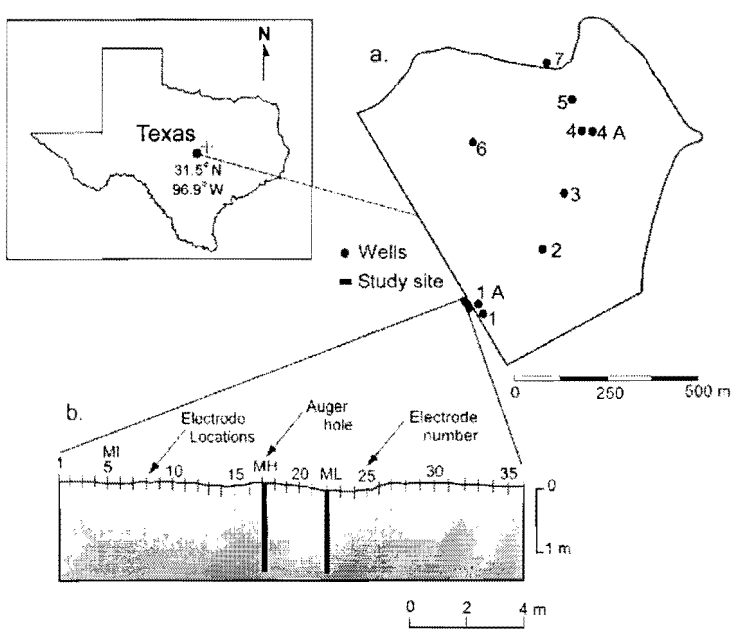

FIG. 1. Study location: (a) location map of USDA Grassland Soil and Water Research Station, near Riesel, TX, showing the study site and distribution of monitoring wells within the station; and (b) sectional view of the experimental layout (MH = microhigh, ML = microlow, MI = intermediate microrelief). The electrodes are numbered 1 to 36.

Archie's law assumes that all current is conducted through the pore fluid, and grain and air-filled pores are insulators. in clay soils, however, the effects on bulk resistivity of conduction of current along the grain surface of soil have been recognized (Urish, 1981; Taylor and Barker, 2006). To account for the effects of grain surface conduction, Archie's (1942) model has been modified to yield parallel-resistor models to describe the soil material–resistivity system for clay soils. A simplified form of these models is given by (Frohlich and Parke, 1989):

$$\frac{1}{\rho_b} = \frac{\Phi^m S^n}{a\rho_w} + \frac{1}{\rho_s} \quad [2]$$

where ρ_b is the soil bulk resistivity and ρ_s, which represents the effects of grain surface conduction, is the resistivity of the grain matrix surfaces. From Eq. [2], it is observed that at high saturation, pore-water resistivity contributes more to the overall bulk resistivity, whereas grain surface conduction becomes important as saturation and grain size decrease. At any soil moisture content, however, the two parameters contribute to the overall bulk resistivity of the soil. Also, at different degrees of saturation (S), measurements of ρ_b incorporate other parameters (soil-water resistivity, porosity, and grain surface conduction) in the equation; however, these other parameters are relatively constant during a wetting and drying cycle. Thus, in theory, measurement of ρ_b at different values of S can be used to characterize temporal variability in soil-water content.

Electrical resistivity techniques are based on the assumption that the subsurface is a continuum—a closely connected metric space (Loke, 2000a). Variation in soil moisture is characterized by relatively smooth variations in resistivity on the inverted resistivity sections (Zhou et al., 2001). On the other hand, cracks in soils (which are normally filled with air) represent resistant structures in terms of electrical prospecting (Samouëlian et al., 2003). They act as small regions within the soil in which values of S and $1/\rho_s$ are zero. This blocks the flow of current and causes it to follow a more circuitous path between electrodes. Hence, the presence of cracks along a current flow path breaks the continuum and thereby results in high values of ρ_b in the soil. In this study, following Samouëlian et al. (2003), cracks in the Vertisol are identified as isolated spots of high-resistivity values on the inverted resistivity sections and of near-zero soil moisture values on the corresponding soil moisture sections.

Field Surveys

Multielectrode resistivity surveys were performed in the study area from 1 May 2005 to 22 Apr. 2006, using a Sting R1/Swift resistivity system (Advanced Geosciences, Austin, TX). The system consists of a portable earth resistivity meter with a Swift control unit and smart electrodes for total automation of the measurement sequence for the array of electrodes. For this study, there were six cables each with two electrode take-outs, and surveys were conducted with the roll-along technique (Advanced Geosciences, 2000). The system was preprogrammed before each field survey for automatic resistivity measurements with dipole–dipole and Schlumberger arrays at a minimum dipole and electrode spacing of 0.5 m. The dipole–dipole array has low electromagnetic coupling between the potential and current circuits and is most sensitive to horizontal changes in resistivity, whereas the Schlumberger (along with Wenner) array is most sensitive to vertical changes in resistivity (Loke, 2000a; Furman et al., 2003; Dahlin and Zhou, 2004). With this combined-array technique, we hypothesized that vertical and horizontal changes in resistivity would be optimally resolved. The resistivity system also has an algorithm for carrying out a resistance test to ensure that the electrodes are in good contact with the soil. This was performed before each field survey to ensure good data quality. We used four-cycle stacking and set the standard error of measurements to 5% in the instrument. With this setting, each measurement was repeated four times and readings that did not agree to within 5% were rejected.

A total of 32 profiles was collected during the study period. The resistivity profiles were 17.5 m long and intersected two sets of microhighs and microlows. Typically, for each field survey, 382 apparent resistivity (a representative resistivity of a volume average of the soil's half-space) readings were collected in a period of about 2 h (249 readings for dipole–dipole array and 133 for Schlumberger array). Surveys were repeated following some of the substantial rain events (>10 mm) at intervals of 1 d, until negligible changes in resistivity were observed on successive surveys. For surveys following rain events, delay times of at least 12 h were allowed before conducting surveys. This was done to ensure that errors due to streaming potentials were negligible in the resistivity readings (Telford et al., 1976). For periods with no rain events, surveys were typically performed at 1-wk intervals. To ensure that the same section was surveyed each time, the electrodes were left in the ground throughout this study. This was particularly important because of the close-interval variability in physical and chemical properties of the soil (Wilding et al., 1991). Also, driving the electrodes in and pulling them out in nearly the same location 33 times would substantially change the near-surface soil properties, due to physical damage to the soil. We surveyed the microrelief topography using a laser-type elevation survey and depths to the water table in the nearby wells, and rain-gauge readings were measured and recorded. Finally, to evaluate resistivity results, auger samples were collected on 23 Mar. 2006 at two sampling points. The sampling points were located adjacent to the profile within a microbigh at 0.2 m from electrode no. 17, and within a microlow at 0.2 m from electrode no. 22 (Fig. 1).

Inversion of Field Resistivity Data and Temperature Corrections

To obtain the true two-dimensional distribution of soil resistivity, the apparent resistivity data were inverted using the program RES2DINV (Loke and Barker, 1996), and the calculated resistivity values were corrected for the effects of temperature. The RES2DINV is a computer program that automatically determines a two-dimensional resistivity model of the subsurface for the input—apparent resistivity data. The program uses an array of rectangular blocks to model the subsurface, and by an iterative forward modeling and correction scheme, calculates resistivity values that agree with the actual measurements. There are two options for data inversion in the program: a rapid least-squares technique (DeGroot-Hedlin and Constable, 1990; Loke and Barker, 1996), which is preferable when there is smooth variation in resistivity in the subsurface; and a robust inversion method (Claerbout and Muir, 1973), which is more applicable to situations involving abrupt changes in resistivity

between adjacent blocks in a medium (Olayinka and Yaramanci, 2000). We used both options in our data inversion, the former to account for smooth variations in resistivity with water content and the latter to account for sharp resistivity gradients due to the effect of cracks in the resistivity data (Samouëlian et al., 2003). The data sets for each array (Schlumberger and Dipole-dipole) were first inverted separately using the rapid least-squares inversion routine. The outputs were then combined using the "general array" option in the program, and were inverted as a single data set using the robust inversion method. The topography was incorporated into the inversion scheme by taking x-(electrode locations) as true horizontal distances. We used the "finite element method with uniform distortion" option in the program for the topographic modeling (Loke, 2000b; Tong and Yang, 1990). By default, the "general array" option uses an extended model where the model blocks extend to the edges of the survey line (Loke, 2000b). The program generated a five-layer model with a total of 175 blocks arranged in 35 blocks per layer. To generate an arrangement of the model blocks such that an individual block does not have sensitivity values that are too small, the option "generate model blocks" was used. The final model sections from the robust inversion were clipped at the edges however, to remove areas still characterized by small sensitivity values where there were not enough data to represent actual resistivity variations in the soil. The inverted data were saved in *XYZ* formats. These contained the coordinates of the model blocks with the inverted resistivity values as well as absolute errors from the robust inversion method. Further details of the inversion scheme are described by Loke (2000a, 2000b).

Following the data inversion, temperature correction was performed. For resistivity measurement during a prolonged period, as in this study, the effect of temperature variation must be accounted for in the resistivity data. Measurements are usually expressed to a reference temperature of 25°C (Rein et al., 2004; Samouëlian et al., 2005). The procedure for temperature correction in this study follows Rein et al. (2004). Hourly soil temperature data at the site were obtained from the USDA database. The data consisted of soil temperature averaged for 0.015- to 0.085-m depth in the soil. We assumed these values are equal to soil temperature at the median depth of 0.05 m. Variations of temperature with depth relative to the 0.05-m depth were then calculated, assuming a sinusoidally varying daily soil temperature, as (Campbell and Norman,1998; Hillel 1998)

$$T(z) = T_a + T_{amp} \exp\left(\frac{-z}{D}\right)\sin\left[\omega(t-8) - \frac{z}{D}\right] \qquad [3]$$

where $T(z)$ is soil temperature at depth z; T_a is the daily average of soil temperature; T_{amp} is the amplitude (half the difference between the maximum and minimum) of the daily soil temperature fluctuations; t is the time of observation reckoned from the zero hour of the day; ω is the angular velocity of earth's rotation (7.3×10^{-5} rad/s) and $D = 2k/\omega$ is the damping depth fot a diurnal wave, where k is the thermal diffusivity of the soil (obtained from Campbell and Norman, 1998). The mean hourly temperature data were used to obtain T_a and T_{amp}, and t is the time of the day surveys were performed (averaged for about 2 h). Generally, Eq. [3] allows variation of temperature with depth to be predicted without necessarily destroying the structure of the soil (Fig. 2). The calculated temperature values were used to correct the inverted resistivity values to 25°C using the equation (Keller and Frischknecht, 1966; Besson et al., 2004)

$$\rho_{25°C} = \rho_T\left[1 + 0.025\left(T - 25°C\right)\right] \qquad [4]$$

where the value 0.025 is the temperature coefficient, and ρ_T and $\rho_{25°C}$ represent resistivity values at temperature T and the reference temperature of 25°C, respectively.

Laboratory Calibration

To calibrate the field results, variations of resistivity with soil-water content were measured in the labotatory. An important issue in laboratory calibrations is that the volume of soil measured in the laboratory is always small compared with the volume measured in the field (Zhou et al., 2001; Michot et al., 2003). Thus, the inevitable but challenging scale transfer or multiscale transfer issue remains at the heart of many hydrologic and pedologic studies (Lin, 2003). In our laboratory calibration, we aimed at reducing errors due to: (i) edge effects on resistivity measurements arising from the finite extent of the soil samples; (ii) deviation from the assumption of a point source of current in the operating principles, and electrode sample coupling—these effects are significant and need to be accounted for in data obtained from resistivity surveys with electrode spacings <1.0 m (Zhdanov and Keller, 1994); and (iii) soil shrinkage with a decrease in soil moisture, which is an important characteristic of the soil under study (Yule and Ritchie, 1980a, 1980b). To account for the edge effects, preliminary measurements were made in a water-filled plastic bucket 30.5 cm in diameter and 15.2 cm deep (this was the anticipated size of the soil samples to be collected). The conductivity of the water in the bucket was increased by adding salt and resistivity values were mea-

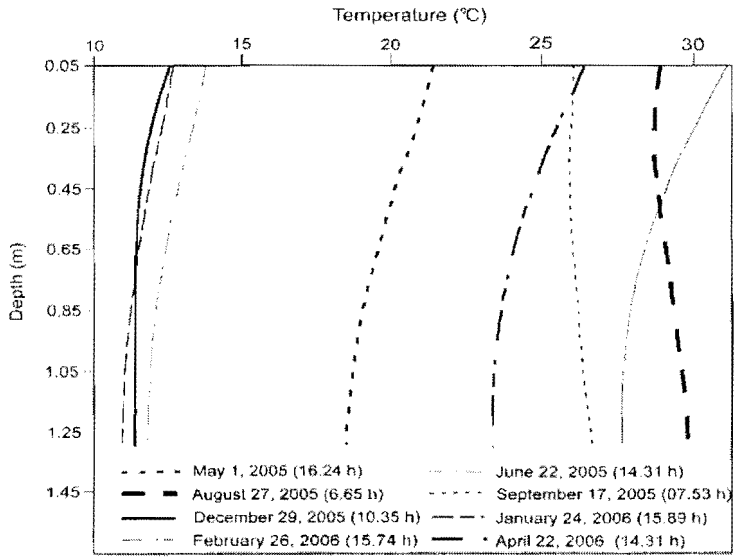

FIG. 2. Examples of estimated temperature profiles in the Vertisol that were used for temperature corrections of the inverted resistivity data. The times indicated on the plot correspond to the average of the time span of resistivity surveys on each day.

sured with the Sting R1 equipment (set up in the manual mode [Advanced Geosciences, 2000]), and a calibtated YSI Model 30 conductivity meter (YSI, Yellow Springs, OH). The water temperature was simultaneously measured with the YSI conductivity meter. For resistivity measurements with the Sting R1 equipment, a Wenner array with four electrodes spread at 8 cm was used. This electrode separation incorporated a greater portion of the water volume in the measurements. The resistivity meter has an accuracy of up to 1% (Advanced Geosciences, 2000), and by using it for both field and laboratory measurements in this study, systematic errors are presumably reduced in the calibration results. The water in the bucket was thoroughly stirred at each stage of the experiment, and thus the medium was assumed homogenous. After corrections of readings to 25°C using Eq. [4], the following relationship was established:

$$\rho_T = 0.6275\rho_W - 0.0536 \quad [5]$$

where ρ_T is the presumed true resistivity of the medium as measured using the YSI conductivity meter and ρ_W is the apparent resistivity value measured using the Wenner array.

Three cylindrical soil samples were collected from the gilgai elements (microlow, microhigh, and intermediate microrelief). The samples were 30.5 cm in diameter and 15.2 cm thick. The soil samples were initially soaked in distilled water for 5 d. They were then drained and four electrodes spread at 8 cm were inserted into the samples (Fig. 3). Then measurements were made using Wenner arrays at different water contents, as the sample dried at room temperature. The insertion of electrodes into the soil samples from the surface and the use of a collinear (Wenner) array in the laboratory measurements were done to approximate the field experiment conditions, and thereby account for deviations from the assumptions of point source of current and electrode sample coupling in the resistivity measurements. Also, because of the relatively large size of the samples, we assumed that the partitioning of the water content was similar to field conditions. The apparent resistivity values (after temperature corrections) were converted to true resistivity values using Eq. [5]. To account for the shrinkage of the soil sample with a decrease in soil moisture, sample volume and bulk density were measured at each stage of the soil drying. The bulk density values were then used to obtain corresponding volumetric soil-water content.

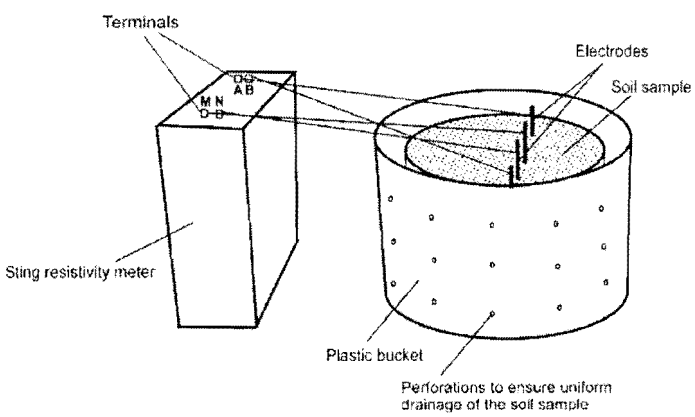

FIG. 3. Experimental setup for the laboratory measurement of resistivity variations with soil moisture.

Next, we established a resistivity–soil moisture relationship for the Vertisol by fitting a modified form of the power-law relation of Yeh et al. (2002) to the laboratory data. Yeh et al. (2002) related bulk electrical resistivity to water content for some sandy soils as follows:

$$\rho_b = \rho_0\theta^{-m} \quad [6]$$

where ρ_b and θ are bulk soil electrical resistivity and soil moisture, as defined previously, ρ_0 is a fitting parameter that is related to the electrical resistivity of pore water, and m is a dimensionless constant. In establishing a fit to our laboratory data, we made θ the dependent variable. This power-law relation eliminates the required and often ill-posed problem of estimating the petrophysical parameters in using Eq. [2] for estimating soil moisture from resistivity data (Zhou et al., 2001). Detailed discussion of the validity of this approach has been presented by Yeh et al. (2002) and Liu and Yeh (2004). Similar approaches have been used by other researchers in similar studies (Walker and Houser, 2002; Hymer et al., 2000; Amer et al., 1994).

Results

Resistivity–Soil Moisture Relationship

Figure 4 shows the resistivity–soil moisture characteristics of the soil samples obtained from the laboratory calibration, and a general curve fitted to the data. Generally, at high water content (>0.5 m^3/m^3), large changes in soil moisture cause small changes in resistivity, whereas at the other extreme (soil moisture <0.18 m^3/m^3), small changes in soil moisture result in large changes in resistivity values. At intermediate soil moisture values, resistivity decreases proportionately with a decrease in soil moisture. It should be noted, however, that the lowest soil moisture value determined was 0.13 m^3/m^3. Below this value, the soil cracked continuously and eventually crumbled, such that no current could be injected into the soil samples.

Further analysis of Fig. 4 shows that the general trend of resistivity and soil moisture variations, especially at higher water content, differs by position within the microrelief. For the same soil moisture values, resistivity values are highest for the microhigh soil sample and lowest for the soil sample collected from

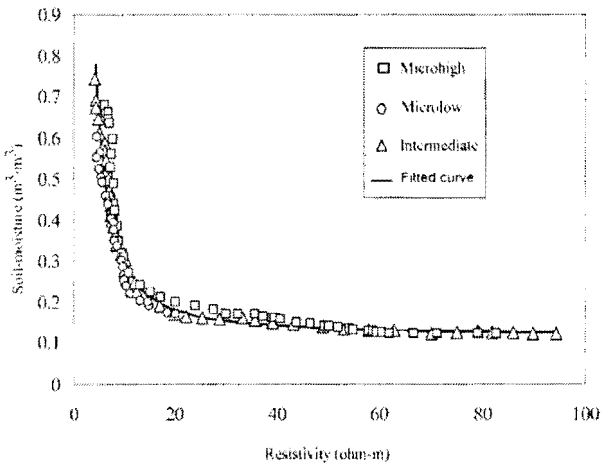

FIG. 4. Soil moisture–resistivity characteristics of the Texas Vertisol.

the microlow. The values for the intermediate microrelief soil lie mostly between these two extremes. For example, at a soil moisture of 0.5 m^3/m^3, resistivity is 6 Ω-m for microlow, 7 Ω-m for intermediate, and 10 Ω-m for microhigh soil samples. The general curve fitted to the data (Fig. 4) is expressed as

$$\theta = 6.0145\rho_b^{-1.536} + 0.12 \quad [7]$$

where the constants in the equation were chosen to optimize the fit in a least-square sense. The first term on the right-hand side is equivalent to the term in Eq. [6]. The added value of 0.12 was used to establish a better fit to the data. We achieved an overall root mean square error of 6.18%.

Field Rainfall Data

Figure 5 shows the rainfall distribution during the period of study. The month of May 2005 was characterized by 8 d of rainfall, with a mean monthly value of 3.33 mm. In June and July 2005, there was cessation in rainfall, which resulted in mean values of 0.43 and 0.9 mm, respectively, for the months. The wettest month during the period of study was August 2005, with average rainfall of 8 mm. From September to December 2005, the average monthly rainfall was mostly <1.0 mm, the lowest monthly average of 0.08 mm being recorded in November 2005. From 22 Jan. 2006, the average monthly rainfall started to rise again. Throughout this study, the depths to the water table were >6 m.

Resistivity-Derived Soil moisture Sections

Figures 6, 7, and 8 show representative soil moisture sections inferred from corresponding resistivity profiles. In deriving the soil moisture values, the temperature-corrected resistivity values of the inverted model blocks were substituted for ρ_b in Eq. [7]. Thus, the soil moisture sections are shaped after the geometry of the inverted resistivity models (Michot et al., 2003). The lateral extent and boundaries of the gilgai elements are shown on the sections. As reported by Zhou et al. (2001), these sections are indicative of relative variations in soil moisture rather than absolute values. Hence, they are hereafter referred to as *apparent soil moisture* sections. These apparent soil moisture sections are divided into three groups and are arranged in the order in which individual field surveys were performed. Each group corresponds to a wetting or drying cycle in the soil. The wetting cycle corresponds to intervals of time on the scale of months, in which there was a net increase in the apparent soil moisture. Conversely, during the drying cycle, there was a net decrease in the apparent soil moisture across the same time scale. Both cycles are characterized by multiple short-term, wetting and drying events on the scale of days.

There are two wetting cycles corresponding to the time intervals from 1 May to 16 Aug. 2005, and from 22 Jan. to 22 Apr. 2006, when the average monthly rainfall was relatively high. They are designated as Wetting Cycles 1 and 2, respectively. The time interval from 16 Aug. 2005 to 22 Jan. 2006, when the average monthly rainfall decreased considerably, corresponds to the drying cycle. The various intervals are indicated in Fig. 5. For the sake of comparison, the resistivity scales as well as absolute errors of data inversion are shown in the sections. Generally, the sections obtained during the wetting cycle are characterized by relatively small absolute errors ranging from 1.9% for the section collected on 1 May 2005 (Fig. 6a) to a value of 5.7% for the data collected on 20 July 2005 (Fig. 6f). The errors for the data collected during the drying period were higher, the highest value of 6.9% being from the data collected on 28 Oct. 2005 (Fig. 7e). It is evident that for the latter, the higher error values are due, in part, to high contact resistance and the presence of cracks in the soil.

Wetting Cycle 1 (Late Spring and Summer 2005)

Figure 6 displays the representative apparent soil moisture–inverted resistivity sections collected in the Vertisol during a wetting cycle in the late spring and summer of 2005. Figure 6a shows that, for the profile collected on 1 May 2005, following a cumulative rainfall of 14.73 mm in April (as inferred from rainfall records preceding this study), apparent soil moisture values vary from about 0.25 to about 0.45 m^3/m^3 from 0- to about 0.5-m depth, and there is spatial variation in apparent soil moisture underneath each of the microrelief elements in this zone. Underlying this layer is a relatively saturated layer with apparent soil moisture mostly greater than about 0.45 m^3/m^3, which extends from about 0.5- to 1.1-m depths. Below about 1.1-m depths, apparent soil moisture varies from about 0.25 to about 0.45 m^3/m^3. These apparent soil moisture–layer relationships are also observable in the profile collected on 24 May 2005 (Fig. 6b), but with pronounced development of isolated spots of lower apparent soil moisture (less than about 0.25 m^3/m^3) at, for example, positions of 5, 8, and 12 m along the profile, in the upper layer. This is indicative of localized drying as a result of no rainfall in the 10-d period before the survey (Fig. 5). Localized lower apparent soil moisture zones are also observable at posi-

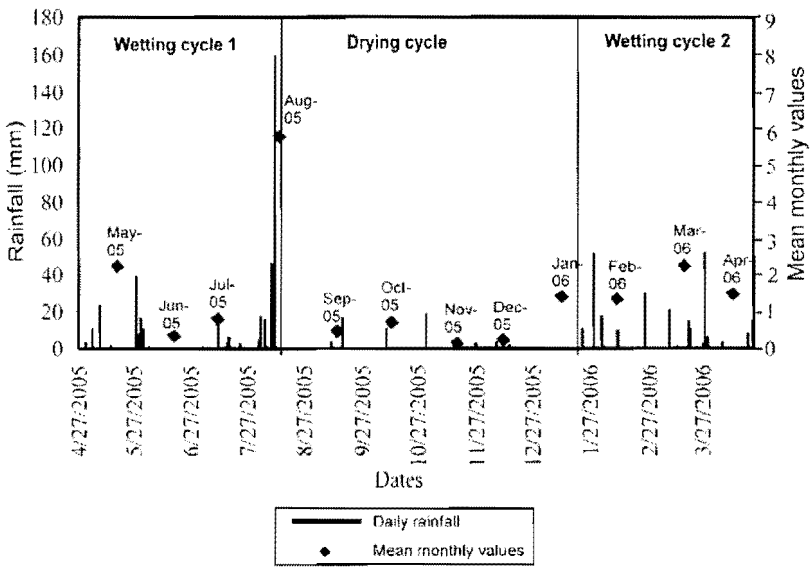

FIG. 5. Rainfall distribution during the period of study. The intervals corresponding to the wetting and drying cycles in the soil are indicated in the figure.

tions 4 and 8 m along the profile, in the lower layer (below about 1.0-m depth).

In the time interval between 9 and 27 May 2005, there were no significant rain events (except for a rain event of 2.03 mm on 14 May 2005; Fig. 5); this led to development of the first set of cracks in the Vertisol. The locations of these cracks were confirmed by visual inspection on 25 May 2005. Figure 6c shows the inverted resistivity–apparent soil moisture section for the profile collected on 29 May 2005 following a rainfall of 39.9 mm on 28 May 2005. The upper 0.2 m, and the depth intervals between about 0.6 and about 1.1 m of the soil are characterized by apparent soil moisture values greater than about 0.5 m^3/m^3, whereas apparent soil moisture variations in the depth intervals between about 0.2 and about 0.5 m, and sections of the soil at depths in excess of about 1.1 m, range from about 0.45 to about 0.3 m^3/m^3. In addition, traces of isolated low apparent soil moisture spots can be noted in the upper layer, with preferential saturation of the regions immediately underlying each spot (corresponding to the points marked "P"). The apparent soil moisture variations in Fig. 6d (the profile collected on 15 June 2005) are similar to those of Fig. 6c, but, because there was no rainfall from 4 to 15 June 2005 (Fig. 5), the thin, relatively saturated layer in the upper 0.2 m in Fig. 6c is no longer visible in Fig. 6d. For the profile collected on 22 June 2006 (Fig. 6e), the pattern of apparent soil moisture variations is similar to those of Fig. 6a and 6b, but, due to further cessation of rainfall in this period (Fig. 5), there are relatively low apparent soil moisture values for the respective sections of the soil. For example, apparent soil moisture values are mostly less than about 0.25 m^3/m^3 in the upper 0.5 m and there is development of isolated low apparent soil moisture spots at, for example, positions 5.5 and 8 m along the profile. Similarly, because the average rainfall between 22 June 2005 and 20 July 2005 was only 0.86 mm, there is a relatively low value of apparent soil moisture for the respective sections of the soil in Fig. 6f (the profile collected on 22 July 2005), when compared with Fig. 6e. The isolated low apparent soil moisture spots in the upper layer of the soil are more developed and the relatively saturated middle layer is less continuous. Figure 6g shows the apparent soil moisture section for the profile collected on 16 Aug. 2005 following the peak rainfall event on 10 Aug. 2005 (Fig. 5). This section reflects a relatively complete saturation of the soil by a cumulative rainfall (from a previous survey) of 212 mm (Fig. 5). As shown in Fig. 6g, apparent soil moisture is mostly greater than about 0.45 m^3/m^3 in the entire section, except for the portions at depths below 1.1 m, where apparent soil moisture is less than about 0.45 m^3/m^3.

Drying Cycle (Fall and Winter 2005–2006)

The representative apparent soil moisture–inverted resistivity sections collected during the drying cycle are shown in Fig. 7. The figure shows depletion in apparent soil moisture, which was initially gradual (Fig. 7a–c) and later became rapid (Fig. 7d–g), after a relatively complete saturation of the soil (Fig. 6g). Because of lack of rainfall between 16 and 27 Aug. 2005 (Fig. 5), apparent soil moisture values in the section collected on 27 Aug. 2005 are mostly less than about 0.3 m^3/m^3 in the upper 0.5 m of the soil in Fig. 7a. There is a relative saturation of the middle layer (about 0.5- to 1.1-m depths),

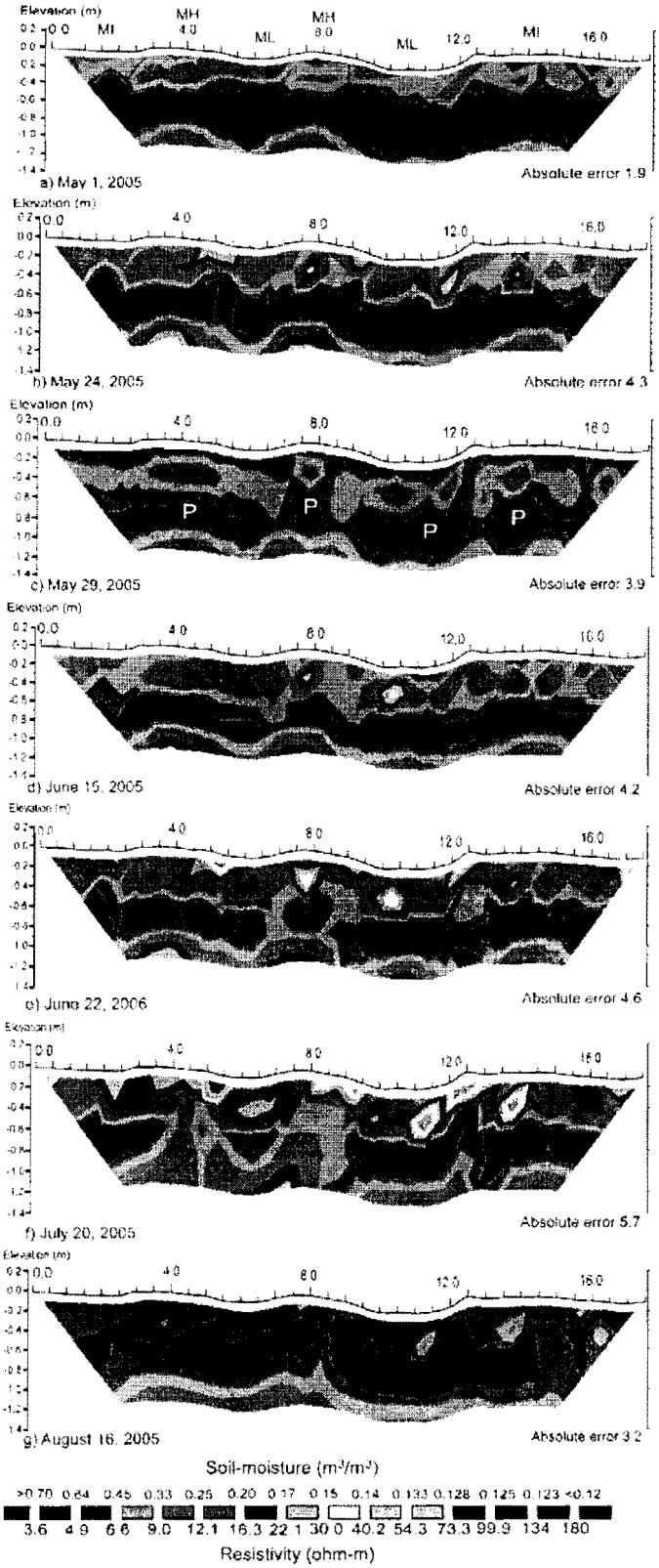

FIG. 6. Representative apparent soil moisture–inverted resistivity sections collected during Wetting Cycle 1 in the Vertisol: (a) 1 May; (b) 24 May; (c) 29 May; (d) 15 June; (e) 22 June; (f) 20 July; and (g) 16 Aug. 2005. The lateral extent of the microhighs (MH), microlows (ML), and the intermediate microrelief (MI) are shown in Fig. 6a. The areas marked "P" in (c) denote preferentially saturated portions of the soil in the section. The absolute error values refer to the errors in % from the robust inversion of the apparent resistivity data.

however, with apparent soil moisture greater than about 0.45 m^3/m^3. At depths >1.1 m in the soil, there is spatial lateral variation in apparent soil moisture but with values mostly less than about 0.3 m^3/m^3. Similar variations in apparent soil moisture are observed in Fig. 7b (the profile collected on 9 Sept. 2005) and Fig. 7c (the profile collected on 17 Sept. 2005) but with relatively low apparent soil moisture values for the respective sections of the soil. Due to a cumulative rainfall of 21 mm in the interval, however, the isolated low apparent soil moisture spots in the upper layer are less visible in Fig. 7c than in Fig. 7b.

The interval from 17 Sept. to 8 Oct. 2005 was characterized by lack of rainfall (Fig. 5). In Fig. 7d (the 8 Oct. 2005 profile), the upper 0.4 m of the soil is dry, with apparent soil moisture values of less than about 0.2 m^3/m^3. In the middle layer, the regions underneath the microlows are of higher apparent soil moisture (greater than about 0.33 m^3/m^3) than the regions underneath microhighs (mostly less than about 0.25 m^3/m^3). At depths in excess of about 1.0 m in the soil, there is spatial variation in apparent soil moisture, with values mostly less than about 0.3 m^3/m^3. Similar apparent soil moisture variation is observed on other profiles collected during this period (Fig. 7e–g), but because the lowest average monthly rainfall was in this period (Fig. 5), there are lower values of apparent soil moisture and more pronounced development of the isolated low apparent soil moisture (high-resistivity) spots, in the subsequent sections.

Wetting Cycle 2 (Winter and Spring 2006)

Figure 8 shows the representative apparent soil moisture–inverted resistivity sections collected following resumption of rainfall events after intense drying of the Vertisol. In Fig. 8a (apparent soil moisture section collected on 24 Jan. 2006), the soil is relatively dry. In comparison with Fig. 7g (apparent soil moisture section collected on 29 Dec. 2005), however, apparent soil moisture values are relatively high in the corresponding portions of the soil due to cumulative rainfall of 11.43 mm in the interval between the two field surveys. As a consequence, the isolated low apparent soil moisture regions in the upper layer are less visible in Fig. 8a than in Fig. 7g.

Figure 8b shows the profile collected on 4 Feb. 2006 following a cumulative rainfall of 70 mm (Fig. 5) 12 d from the previous survey on 24 Jan. 2006 (Fig. 8a). There is relative saturation of the upper 0.3 m of the soil, with the inferred apparent water-content values greater than about 0.45 m^3/m^3; however, isolated spots of near-zero apparent soil moisture, especially at the position 7 m along the profile in the upper layer, could still be observed. The lower portions at depths below about 0.4 m are characterized by apparent soil moisture mostly less than about 0.45 m^3/m^3. With an increase in cumulative rainfall (Fig. 5), progressive movement of the wetting front down to deeper sections of the soil could be observed on subsequent sections (Fig. 8c–8f). Also, relicts of the isolated low apparent soil moisture spots are visible in the upper 0.4 m of the soil.

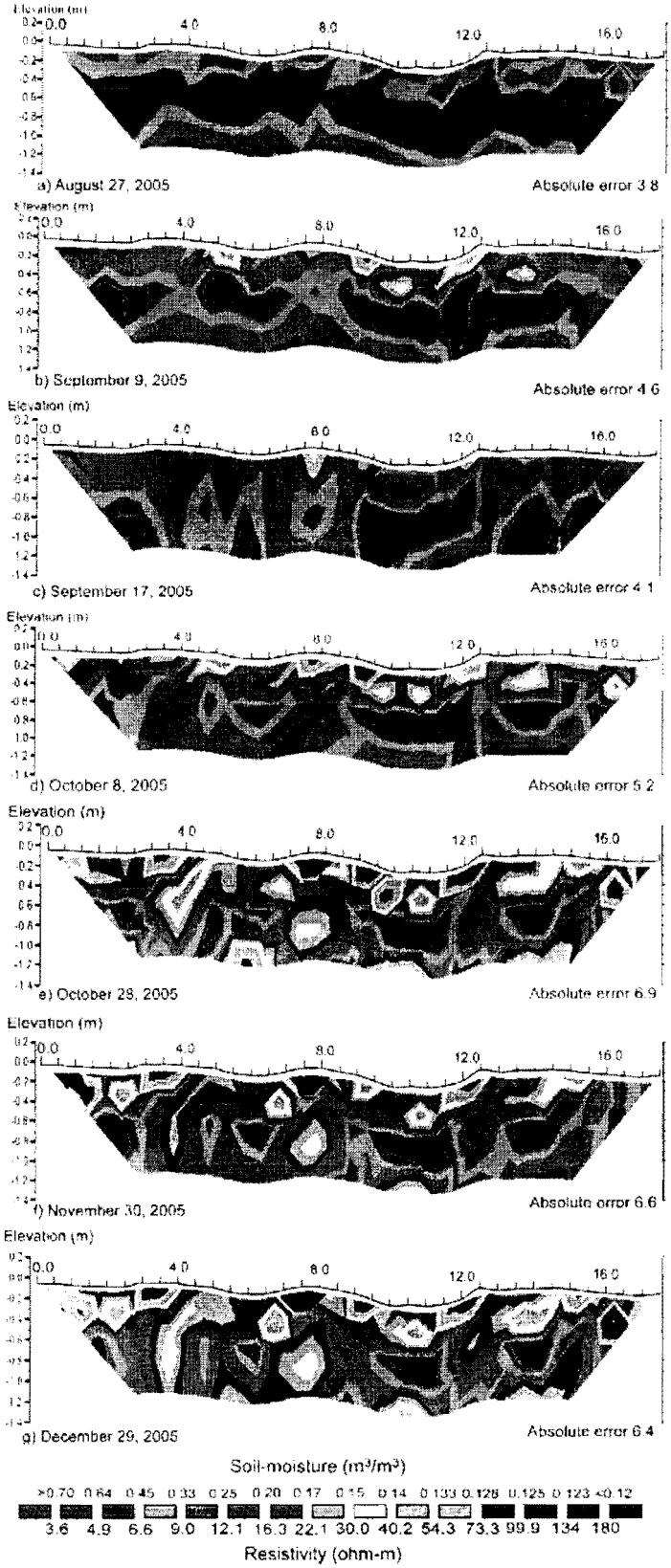

FIG. 7. Representative apparent soil moisture–inverted resistivity sections collected during the drying cycle in the Vertisol: (a) 27 August; (b) 9 September; (c) 17 September; (d) 8 October; (e) 28 October; (f) 30 November; and (g) 29 Dec. 2005. The absolute error values refer to the errors in % from the robust apparent resistivity data inversion.

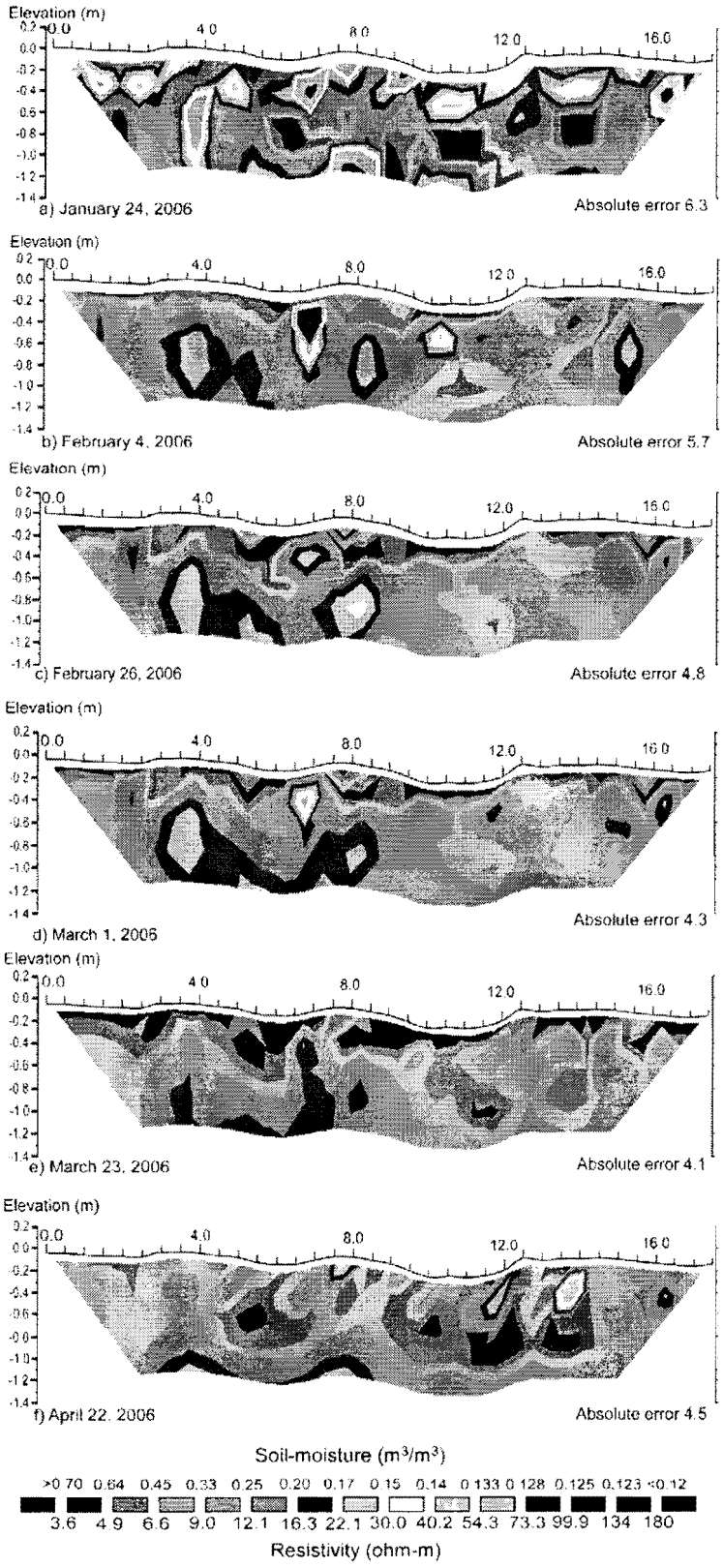

FIG. 8. Representative apparent soil moisture–inverted resistivity sections collected during Wetting Cycle 2 in the Vertisol: (a) 24 January; (b) 4 February; (c) 26 February; (d) 1 March; (e) 23 March; and (f) 22 Apr. 2006. The absolute error values refer to the errors in % from the robust inversion of the apparent resistivity data.

Data Evaluation

Figure 9 shows comparisons of the resistivity-derived apparent soil moisture values for the 23 Mar. 2006 survey (Fig. 8e) to the results of auger sampling. The apparent soil moisture values were extracted from vertical variations of apparent soil moisture at 8- and 10.5-m positions along the profile (Fig. 8e), which are the closest points to the microhigh and the microlow auger sampling points, respectively (Fig. 1). Also, in computing the volumetric moisture from gravimetric values obtained for the auger samples, we used soil bulk density values ranging from 1.2 g/cm^3 at the surface, which was at higher moisture content at the time of sampling, to 1.5 g/cm^3 at depth (Coulombe et al., 1996; Plant, 2000). The various data were then interpolated so that results could be compared for the same depths. As shown in Fig. 9a, for the measurements taken within the microhigh, the resistivity-derived apparent soil moisture values are lower than soil moisture values derived from auger sampling by an average of about 16% in the upper 0.2 m of the soil. From 0.2- to about 0.6-m depth, the apparent soil moisture values are greater than soil moisture derived from auger sampling by about 22%. Below 0.6-m depth, the relationship is essentially the same as in the upper 0.2 m but with an average difference of about 19%. For the sampling within the microlow (Fig. 8b), the apparent soil moisture values are highest in the upper 1.0 m by an average of about 17%, whereas at greater depths, the values are lower than soil moisture obtained from auger sampling by about 14%.

Discussion

Soil Moisture–Resistivity Characteristics of the Vertisol and Data Evaluation

The resistivity–soil moisture relationships for the Vertisol obtained from laboratory measurements (Fig. 4) follow the trend for clay soils (McCarter, 1984; Samouëlian et al., 2005). At high soil moisture, it is probable that current conduction is mainly through the pore water, whereas current conduction along the grain surfaces probably predominates at low water content in the Vertisol. At the intermediate soil moisture values, the proportionate decrease in resistivity with soil moisture shows resultant effects of conductivity due to the pore water in the conduits and the matrix conductivity along grain surfaces. In Eq. [7], the value of 0.12 added to the optimization scheme probably denotes the effects of current conduction along the grain surfaces analogous, but not necessarily equal, to the effects of $1/\rho_s$ in Eq. [2]. This value may be equivalent to the water content near which it is impossible (or at least difficult) to inject current to estimate soil moisture in the Vertisol using the approach presented in this study. Presumably, near this value in the apparent soil moisture sections (Fig. 6, 7, and 8), the inferred soil moisture is influenced primarily by cracks in the soil.

The trends in soil moisture from data evaluation in Fig. 9 indicate that, for the most part, the values of the resistivity-measured apparent soil moisture are greater than soil moisture values derived from auger sampling at relatively high water content, whereas at relatively low water content, the values are smaller. The exception is shown in Fig. 9a, where apparent soil moisture values are lower than soil moisture derived from the auger sampling at relatively high water content in the upper 0.2 m of the soil. The difference between the apparent soil moisture and soil moisture derived from auger sampling may be due to close-interval variability in physical and chemical properties of the soil (Wilding et al., 1991; Akbar et al., 2004), and the fact that the resistivity measurements were calibrated according to the surface soil, whereas soil profiles in Vertisols are known to change significantly in pedological properties with depth (Wilding et al., 1991; Nordt et al., 2004). The relatively low value of the resistivity-derived apparent soil moisture in the upper 0.2 m in Fig. 9a may be due to the effect of a probable crack around the 8-m position along the profile (Fig. 8c). Additional difference may, however, be due to ambiguity implicit in the two-dimensional approximation of three-dimensional flow of current in the resistivity survey, as well as artifacts in the resistivity data inversion scheme (Zhou et al., 2001). Nevertheless, because the general trends of the apparent soil moisture followed, to some extent, the soil moisture measured by the auger sampling (especially as shown in Fig. 9b), we conclude that the resistivity-derived apparent soil moisture data are valid for characterization of seasonal wetting and drying of this Vertisol, which was the main objective of this study.

Characterization of Seasonal Wetting and Drying

The geoelectric study of seasonal wetting and drying of this Texas Vertisol revealed the spatiotemporal pattern of soil-water variations in the soil. The wetting and drying of the Vertisol correlate with rainfall distribution in the area (Fig. 5) and are influenced by cracking and microrelief variability. As shown in Fig. 6, the upper 1.4 m of the soil can be divided into three soil moisture regimes: an upper zone (from 0- to about 0.5-m depth), which is of relatively low soil moisture; a middle zone (from about 0.5- to about 1.1-m depth), which is relatively saturated; and the lower zone (below about 1.1-m depth), which is relatively less saturated than the middle layer. The upper layer is the interface between the atmosphere and the deeper sections and, as expected, is the most dynamic with regard to wetting and drying in the Vertisol. The saturation of the middle layer appears to be enhanced by bypass flow into the deeper sections of the soil. For example, as can be inferred from Fig. 6c, the portions of soil presumably underneath the cracks (localized spots of high resistivity and low apparent soil moisture) are preferentially saturated relative to other areas in the Vertisol. According to Lin et al. (1997), bypass flow through cracks may constitute an important mechanism that may lead to rapid transport of contaminants to groundwater. Also, according to Allen et al. (2005), rapid recharge in the study area is related to bypass flow. Even when the soil surface approaches field capacity, the remaining cracks are sufficient to support flow rates of 2.5 cm/d around the soil structural units (Allen et al., 2005; Ritchie et al., 1972). It can also be inferred that the more intense the rainfall, the greater the preferential flow process in the Vertisol. For example, the relatively complete

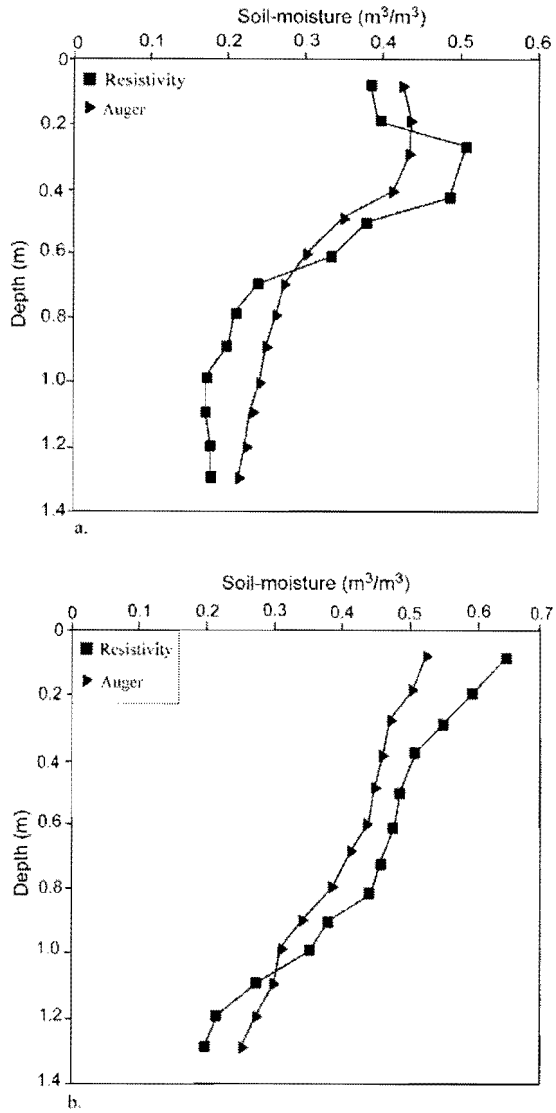

Fig. 9. Comparisons of results of soil moisture values derived from resistivity measurements of 23 Mar. 2006 to those obtained from auger sampling on the same date: (a) measurements within the microhigh; (b) measurements within the microlow.

saturation of the soil as shown in Fig. 6g is enhanced by the rainfall events. Following these events, lateral infiltration probably proceeds at the same rate as vertical movement of water in the soil (Favre et al., 1997). The low hydraulic conductivity of the soil, however, ensures that the lower portion below about 1.2-m depth is still relatively less saturated. In addition, it appears that the localized low apparent soil moisture spots extend to the soil surface in the profiles collected following localized drying as a result of cessation of rainfall (Fig. 6b), whereas following rainfall events, they appear closed at the surface with their traces visible at depth in the section (Fig. 6c). Thus, in accordance with the work of Favre et al. (1997), crack closure starts from the soil surface and progresses downward in the soil.

This study also shows that microrelief features exercise a significant control on seasonal variations in soil moisture regimes in the Vertisol. By comparing variations in apparent soil moisture in the various profiles, it can be observed that more moisture

is retained underneath microlows than underneath microhighs throughout the wetting and drying cycles. The relative saturation of the microlows, especially during the wetting cycle, might be due to the fact that much of the rainfall falling on the microhighs runs off into the microlows (Newman, 1986). This is supported by our field observation that more vegetation was produced in the microlows than on the microhighs. In addition, the soils beneath microlows have been known to have higher organic content than those underneath the microhighs (Wilding et al., 1991; Nordt et al., 2004). An implication of this result is that, in a typical farming season, assuming other effects are negligible, crops planted on microlows will give higher yield than those planted on microhighs because of differential availability of water (Wilding et al., 1991) and, by implication, nutrients (Rodriguez-Iturbe, 2000) to the plants. Thus, a consideration of the hydrologic effects of gilgai microrelief is important for optimal agricultural management of Vertisols.

The profiles collected during the drying cycle (Fig. 7) and the beginning of the wetting cycle (Fig. 8a) illustrate cracking patterns in the soil. Although crack geometry and depth cannot be determined precisely from two-dimensional resistivity sections and inversion schemes based on regularized mesh such as RES2DINV (Samouëlian et al., 2003), the distribution of cracks within the upper layer and duration of cracking can be inferred from the apparent soil moisture–inverted resistivity sections. This is particularly important in developing better classification schemes for Vertisols (Wilding et al., 1991; Dudal and Eswaran, 1988; Newman, 1986). As mentioned above, the localized near-zero soil moisture (high-resistivity) spots are interpreted as corresponding to cracks in the upper layer. It can be noted from the sections that more cracks are concentrated on the microhighs and intermediate portions of the soil than in the microlows. This may be correlated to microclimatic variability between the microhigh and microlow features. According to Newman (1986), microhighs and microlows control surface water flow in the same way as larger topographic features. Hence, it is natural that the soil beneath the microhighs would be drier and more intensely cracked than that beneath the microlows. Further analysis of the sections shows that cracks (especially those around distances of 8 and 12 m) opened between 8 Oct. 2005 (Fig. 7d) and 24 Jan. 2006 (Fig. 8a). This is consistent with the classification (NRCS, 2001; Soil Survey Staff, 1999) of the Vertisol under study as belonging to udic–ustic soil moisture regime. This classification requires, in part, that cracks be opened from 90 to 150 cumulative days in most years (Dudal and Eswaran, 1988).

Moreover, it can be inferred from Fig. 8 that rewetting of the Vertisol after intense drying is, among other factors, a function of the amount of rainfall and antecedent moisture content. For example, in Fig. 8b, due to the low antecedent moisture content, the added moisture was absorbed in the upper portions of the soil and, due to the relatively small amount of rainfall, bypass flow was not noticeable underneath the cracks. This is especially true for the apparent crack shown at position of 7.5 m along the profile. Additional rainfall events led to further saturation of the soil, with the cracks being less visible on subsequent sections. In addition, the observed movement of the wetting front into the deeper sections with cumulative rainfall shows that the data from this study can be used for calculating soil moisture flux and flow gradient, which may be important in studying contaminant hydrology of the soil. Additional studies are required, however, to verify this assertion.

This study has shown that electrical resistivity techniques can be effective methods of characterizing hydrological properties and processes in Vertisols. Unlike conventional methods of soil moisrure measurements, the techniques allow cracks and gilgai microrelief features to be incorporated into soil moisture profiles. For resistivity methods to evolve as a tool for routine hydrologic studies of Vertisols, however, improvements in survey designs and data inversion schemes are needed. Further work is recommended in the study area with three-dimensional imaging and time-lapse techniques. It would also be of interest to test other electrode configurations such as square arrays in the laboratory and field measurements. Finally, we did not observe movement of electrodes left in the ground during the field surveys, and they were not observed to have induced cracking in the soil. This might have been due to relatively low lateral flow property of the soil (Allen et al., 2005), which may not be applicable to other Vertisols. Thus, further studies are recommended to investigate if techniques and phenomena reported in this study can be considered applicable to all Vertisols.

Conclusions

In this study, field and laboratory electrical resistivity measurements were used to characterize seasonal wetting and drying of a Texas Vertisol. Laboratory measurements were used to generate soil moisture–resistivity relarionships and to calibrate data from two-dimensional resistivity monitoring of spatiotemporal soil moisture variations in the Vertisol during a period of 1 yr. Both laboratory and field resistivity data were corrected for the effect of temperature variations. The results of resistivity measurements are correlated to the results of soil moisture measurements with auger sampling. The results show that the upper 1.4 m of the Vertisol can be divided into three soil moisture regimes: an upper zone (from 0- to about 0.5-m depth), which is the most dynamic with regard to wetting and drying in the soil; a middle zone (from about 0.5- to about 1.1-m depths), which is relatively saturated during periods of substantial rainfall when the soil is wet; and a lower zone (below about 1.1-m depth), which is relatively less saturated than the middle layer. The saturation of the middle layer appears to be enhanced by preferential flow through cracks into the soil. It is apparent from the resistivity–apparent soil moisture sections that most cracks terminate at depths in this layer. Moreover, the microrelief topography exercises a significant control on spatial and temporal variations in soil moisture in that the microhighs dry out faster than the microlows. This study should be of relevance for better agricultural management of Vertisols.

Acknowledgments

This study was partly funded by the Geological Society of America (Grant no. 8193-06) and by Baylor Geology, O.T. Hayward Field Research Fund, awarded to S.A. Amidu. We acknowledge rhe USDA for allowing access to research facilities at Riesel and Mr. J. Haug and Dr. D. Harmel for assisting with the collection of the rainfall and soil temperature data. We also thank Dr. P.M. Allen, Baylor University, for suggestions that helped improve the quality of this study. Bharath Kumar provided invaluable assistance during the field work. Helpful reviews of earlier drafts of this manuscript by Drs. S.G. Driese, J.D. White, and T. Goforth are appreciated.

References

Advanced Geosciences. 2000. Instruction manual for Sting R1 IP and Swift automatic earth resistivity and IP system. Adv. Geosci., Austin, TX.

Akbar, M.A., A.L. Kenimer, and S.W. Searcy. 2004. Estimating soil profile depth with apparent electrical conductivity for a Texas Vertisol. Trans. ASAE 47:1087–1092.

Allen, P.M., R.D. Harmel, J. Arnold, B. Plant, J. Yelderman, and K. King. 2005. Field data and flow system response in clay (Vertisol) shale terrain, north central Texas, USA. Hydrol. Proc. 19:2719–2736.

Amer, S.A., T.O. Keefer, M.A. Weltz, D.C. Goodrich, and L.B. Bach. 1994. Soil moisture sensors for continuous monitoring. Water Resour. Bull. 30:69–83.

Amidu, S.A., and A.I. Olayinka. 2006. Environmental assessment of sewage disposal systems using 2D electrical-resistivity imaging and geochemical analysis: A case study from Ibadan, southwestern Nigeria. Environ. Eng. Geosci. 12:261–272.

Archie, G.I. 1942. The electrical resistivity log as an aid in determining some reservoir characteristics. Trans. Am. Inst. Min. Metallurg. Eng. 146:54–62.

Besson, A., I. Cousin, A. Samouëlian, H. Boizard, and G. Richard. 2004. Structural heterogeneity of the soil tilled layer as characterized by 2D electrical resistivity surveying. Soil Tillage Res. 9:239–249.

Bouma, J., and J. Loveday. 1988. Characterizing soil water regimes in swelling clay soils. p. 83–96. *In* L.P. Wilding and R. Puentes (ed.) Vertisols: Their distribution, properties, classification, and management. Texas A&M Univ., College Station.

Bussian, A.E. 1983. Electrical conductance in a porous medium. Geophysics 48:1258–1268.

Campbell, G.S., and J.M. Norman. 1998. An introduction to environmental biophysics. 2nd ed. Springer Sci. Business Media, New York.

Claerbout, J.F., and F. Muir. 1973. Robust modeling with erratic data. Geophysics 38:826–844.

Coulombe, C., L. Wilding, and J. Dixon. 1996. Overview of Vertisols: Characteristics and impacts on society. Adv. Agron. 57:289–375.

Dahlin, T., and B. Zhou. 2004. A numerical comparison of 2D resistivity imaging with 10 electrode arrays. Geophys. Prospect. 52:379–398.

Davis, J.L., and A.P. Annan. 1989. Ground-penetrating radar for high resolution mapping of soil and rock stratigraphy. Geophys. Prospect. 37:531–551.

DeGroot-Hedlin, C., and C. Constable. 1990. Occam's inversion to generate smooth two dimensional models from magnetotelluric data. Geophysics 55:1613–1624.

Dudal, R., and H. Eswaran. 1988. Distribution, properties and classification of Vertisols. p. 1–22. *In* L.P. Wilding and R. Puentes (ed.) Vertisols: Their distribution, properties, classification, and management. Texas A&M Univ., College Station.

Favre, F., P. Boivin, and M.C.S. Wopereis. 1997. Water movement and soil swelling in a dry cracked Vertisol. Geoderma 78:113–123.

Frohlich, R.K., and C.D. Parke. 1989. The electrical resistivity of the vadose zone: Field survey. Ground Water 27:524–530.

Furman, A., P.S. Ferre, and A.W. Warrick. 2003. A sensitivity analysis of electrical resistivity tomography array types using analytical element modeling. Vadose Zone J. 2:416–423.

Garambois, S., P. Sénéchal, and H. Perroud. 2002. On the use of combined geophysical methods to assess water content and water conductivity of near-surface formations. J. Hydrol. 259:32–48.

Griffith, D.H., and R.D. Barker. 1993. Two-dimensional resistivity imaging and modeling in areas of complex geology. J. Appl. Geophys. 29:211–226.

Gustavson, T.C. 1975. Microrelief (gilgai) structures on expansive clays of the Texas coastal plain—their recognition and significance in engineering construction. Geol. Circ. 75-7. Bull. of Econ. Geol. Univ. of Texas, Austin.

Hagrey, S.A.A., and J. Michaelsen. 1999. Resistivity and percolation study of preferential flow in vadose zone at Bokhorst, Germany. Geophysics 64:746–753.

Halvorson, A.D., and J.D. Rhoades. 1976. Field mapping soil conductivity to delineate dryland saline seeps with four-electrode technique. Soil Sci. Soc. Am. J. 40:571–575.

Hillel, D. 1998. Environmental soil physics. Academic Press, San Diego.

Hymer, D.C., M.S. Moran, and T.O. Keefer. 2000. Soil water evaluation using a hydrologic model and calibrated sensor network. Soil Sci. Soc. Am. J. 64:319–326.

Keller, G.V., and F.C. Frischknecht. 1966. Electrical methods in geophysical prospecting. Pergamon Press, Oxford, UK.

Lin, H. 2003. Hydropedology: Bridging disciplines, scales, and data. Vadose Zone J. 2:1–11.

Lin, H.S., K.J. McInnes, L.P. Wilding, and C.T. Hallmark. 1997. Low tension water flow in structured soils. Can. J. Soil Sci. 77:649–654.

Lin, H.S., K.J. McInnes, L.P. Wilding, and C.T. Hallmark. 1998. Macroporosity and initial moisture effects on infiltration rates in Vertisols and vertic intergrades. Soil Sci. 163:2–8.

Liu, S., and T.-C.J. Yeh. 2004. An integrative approach for monitoring water movement in the vadose zone. Vadose Zone J. 3:681–692.

Loke, M.H. 2000a. Electrical imaging surveys for environmental and engineering studies. Available at www.geotomals.co.uk/Lokenote.pdf (verified 3 May 2007). Geomatrix Earth Sci., Leighton Buzzard, UK.

Loke, M.H. 2000b. RES2DINV Version 3.44 for Windows 95/98 and NT: Rapid 2D resistivity and IP inversion using the least-squares method. Adv. Geosci., Austin, TX.

Loke, M.H., and R.D. Barker. 1996. Rapid least-square inversion of apparent resistivity pseudosections by quasi-Newton method. Geophys. Prospect. 44:131–152.

McCarter, W.J. 1984. The electrical resistivity characteristics of compacted clays. Geotechnique 32:263–267.

Mermut, A.R., G.S. Dasog, and G.N. Dowuona. 1996. Soil morphology. p. 89–114. *In* N. Ahmad and A. Mermut (ed.) Vertisols and technologies for their management. Elsevier Sci., Amsterdam.

Michot, D., Y. Benderitter, A. Dorigny, B. Nicoullaud, D. King, and A. Tabbagh. 2003. Spatial and temporal monitoring of soil water content with an irrigated corn crop cover using surface electrical resistivity tomography. Water Resour. Res. 39(5):1138, doi:10.1029/2002WR001581.

Natural Resources Conservation Service. 2001. Soil survey of McLennan County, Texas. NRCS, Washington, DC.

Newman, A.L. 1986. Vertisols in Texas—some comments. USDA Soil Conserv. Serv., Temple, TX.

Nordt, L.C., L.P. Wilding, W.C. Lynn, and C.C. Crawford. 2004. Vertisol genesis in a humid climate of the coastal plain of Texas, U.S.A. Geoderma 122:83–102.

Olayinka, A.I., and U. Yaramanci. 2000. Use of block inversion in the 2-D interpretation of apparent resistivity data and its comparison with smooth inversion. J. Appl. Geophys. 45:63–81.

Plant, B. 2000. Recharge in a clay shale terrain: A water budget approach. M.S. thesis. Baylor Univ., Waco, TX.

Rein, A., R. Hoffmann, and P. Dietrich. 2004. Influence of natural time-dependent variations of electrical conductivity on DC resistivity measurements. J. Hydrol. 285:215–232.

Ritchie, J.T., D.E. Kissel, and E. Burnett. 1972. Water movement in undisturbed swelling clay soil. Soil Sci. Soc. Am. Proc. 36:874–879.

Rodriguez-Iturbe, I. 2000. Ecohydrology: A hydrodynamic perspective of climate–soil–vegetation dynamics. Water Resour. Res. 36:3–9.

Saarenketo, T. 1998. Electrical properties of water in clay and silty soils. J. Appl. Geophys. 40:73–88.

Samouëlian, A., C. Isabelle, G. Richard, A. Tabbargh, and A. Bruand. 2003. Electrical resistivity imaging for detecting soil cracks at the centimetric scale. Soil Sci. Soc. Am. J. 67:1319–1326.

Samouëlian, A., C. Isabelle, A. Tabbagh, A. Bruand, and G. Richard. 2005. Electrical resistivity survey in soil science: A review. Soil Tillage Res. 83:173–193.

Soil Conservation Service. 1942. The agriculture, soils, geology, and topography of the Blacklands Experimental Watershed, Waco, TX. Hydrol. Bull. 5. USDA Soil Conserv. Serv., Washington, DC.

Soil Survey Staff. 1999. Soil taxonomy, a basic system of soil classification for making and interpreting soil surveys. 2nd ed. Agric. Handbk. 436. U.S. Gov. Print. Office, Washington, DC.

Tabbagh, A., M. Dabas, A. Hesse, and C. Panissod. 2000. Soil resistivity: A non-invasive tool to map soil structure horizonation. Geoderma 97:393–404.

Taylor, S., and R. Barker. 2006. Modelling the DC electrical response of fully and partially saturated Permo-Triassic sandstone. Geophys. Prospect. 54:351–367.

Telford, W.M., L.P. Geldert, R.E. Sheriff, and D.A. Keys. 1976. Applied geophysics. Cambridge Univ. Press, Cambridge, UK.

Tong, L., and C. Yang. 1990. Incorporation of topography into two-dimensional resistivity inversion. Geophysics 55:354–361.

Urish, D.W. 1981. Electrical resistivity–hydraulic conductivity relationships in glacial outwash aquifers. Water Resour. Res. 17:1401–1408.

Walker, J.P., and P.R. Houser. 2002. Evaluation of the OhmMapper instrument for soil moisture measurement. Soil Sci. Soc. Am. J. 66:728–734.

Wilding, L.P., and R. Puentes. 1988. Vertisols: Their distribution, properties, classification and management. Texas A & M Univ., College Station, TX.

Wilding, L.P., and D. Tessier. 1988. Genesis of Vertisol shrink–well phenomena. p. 55–81. *In* L.P. Wilding and R. Puentes (ed.) Vertisols: Their distribution, properties, classification and management. Texas A&M Univ., College Station.

Wilding, L.P., D. Williams, W. Millar, T. Cook, and H. Eswaran. 1991. Close interval spatial variability of Vertisols: A case study in Texas. p. 232–247. *In* J.M. Kimble (ed.) Characterization, classification, and utilization of cold Aridisol and Vertisols. Proc. Int. Soil Correlation Meet., 6th. 6–18 Aug. 1991. Natl. Soil Surv. Ctr., Lincoln, NE.

Yeh, T.-C.J., S. Liu, R.J. Glass, K. Baker, J.R. Brainard, D. Alumbaugh, and D. LaBrecque. 2002. A geostatistically based inverse model for electrical resistivity surveys and its applications to vadose zone hydrology. Water Resour. Res. 38:1278, doi:10.1029/2001WR001024.

Yule, D.F., and J.T. Richie. 1980a. Soil shrinkage relationships of Texas Vertisols: I. Small cores. Soil Sci. Soc. Am. J. 44:1285–1291.

Yule, D.F., and J.T. Richie. 1980a. Soil shrinkage relationships of Texas Vertisols: II. Large cores. Soil Sci. Soc. Am. J. 44:1291–1295.

Zhdanov, M.S., and G.V. Keller. 1994. The geoelectrical methods in geophysical exploration. Elsevier Sci., Amsterdam.

Zhou, Q.Y., J. Shimada, and A. Sato. 2001. Three-dimensional spatial and temporal monitoring of soil water content using electrical resistivity tomography. Water Resour. Res. 37:273–285.